ISSN 0010-9525, Cosmic Research, 2016, Vol. 54, No. 2, pp. 105–110. © Pleiades Publishing, Ltd., 2016.
Original Russian Text © A.V. Mikhalev, V.V. Khakhinov, A.B. Beletskii, V.P. Lebedev, 2016, published in Kosmicheskie Issledovaniya, 2016, Vol. 54, No. 2, pp. 113–118.

Optical Effects of the Operation of the Onboard Engine of the *Progress M-17M* Spacecraft at Thermospheric Heights

A. V. Mikhalev, V. V. Khakhinov, A. B. Beletskii, and V. P. Lebedev

Institute of Solar–Terrestrial Physics, Siberian Branch, Russian Academy of Sciences, ul. Lermontova 126a, P.O. Box 291, Irkutsk, 664033 Russia

e-mail: mikhalev@iszf.irk.ru

Received May 5, 2014

Abstract—This paper presents the results of optical observations in the active space experiment "Radar-Progress" on April 17, 2013, after switching on the approach-correction engine of the *Progress M-17M* cargo spacecraft at thermospheric heights (412 km), are presented in this paper. During engine operation, a region of enhanced emission intensity has been recorded. It was presumably related to the scatter of twilight solar emission at the engine exhausts in the cargo spacecraft orbit and, probably to the occurrence of an additional emission in the atomic oxygen line [OI] 630 nm. The maximum observed dimensions of the emission region were ~350 and ~250 km along the orbit and across it, respectively. The velocity of the expansion of the emission region at the first moments after the initiation of engine operation was ~7 and ~3.5 km/s along the orbit and across it, respectively. The maximum intensity of the disturbed region is estimated to be a value equivalent to ~40–60 R within the spectral band of 2 nm. No optical manifestation, which would exceed the natural variations in brightness of the night airglow and which would be related to possible large-scale modification of the ionosphere, was detected in the natural emission lines [O] 557.7 and 630.0 nm in a zone remote from the place of injection of engine exhausts.

DOI: 10.1134/S0010952516020039

1. INTRODUCTION

The optical effects of spacecraft flights and the operation of their approach correction engine (ACE) are split, depending on mechanisms, heights, and spatial scales of their manifestation, into several types [1, 6]. The mechanisms of ACE influence on the atmosphere and ionosphere of the Earth accompanied by optical effects are related to the ejections into the atmosphere of combustion products containing gas and dispersed components and the subsequent scattering of the sunlight from them [1]. The mechanisms are also related to the modification of the atmosphere and the ionosphere by the exhaust products of EI [4, 13], and to the hydrodynamic disturbances of the acoustic–gravity wave type [4, 5, 15]. The majority of optical effects were observed at the height of the tropo-stratosphere, where their brightness is relatively high [6].

The results of optical observations in the Radar Progress active space experiment on April 17, 2013 after switching on ACE of the Progress M-17M cargo ship (CS) at thermospheric heights (412 km) are presented.

2. RADAR-PROGRESS ACTIVE SPACE EXPERIMENT

The space experiment entitled "Investigation of ground-based observations of reflection characteristics of plasma irregularities in the ionosphere generated by the onboard engines of the Progress" (code "Radar-Progress") has been underway since 2007. From 2007 to 2010, its code was SE "Plasma-Progress" [17, 18, 8–11]. The participating organizations are: TcNIImash, ISTP SB RAS, and RSC Energia.

The SE "Radar-Progress" is being carried out in stages of autonomic flights of a SC of the Progress series after performing its main mission of bringing cargo to the *International Space Station (ISS)*. The SE session is conducted during SC flight in the survey zone of the Irkutsk Incoherent Scatter Radar (IISR) [12]. ACEs of SC are switched on. Ground-based unique scientific installations and the equipment of the common use center (CUC) Angara of ISTP SB RAS (http://ckp-angara.iszf.irk.ru/html/history.html) are used.

The solar, geophysical, and meteorological conditions are determined during or immediately after the SE session: solar activity, geomagnetic field state, background parameters of the ionosphere, conditions of illumination (solar zenith angle), and cloudiness.

The governing conditions of each SE session are planned in advance; namely the direction of the exhaust jets and the type and duration of the ACE operation. The latter determine the mass of the burned fuel or the amount of combustion products injected into the ionosphere. For example, the ACE used in the

later sessions of SE "Radar-Progress" burns 1 kg of liquid fuel per second. The maximum duration of the ACE switching-on was 11 s. Given such duration, the exhaust products of burning 11 kg of fuel are injected into the ionosphere along the arc of the CS orbit, with a length of more than 80 km. Such weak influences on the ionospheric plasma are comparable by their power with natural disturbances, and the planned conditions of each session are a specific feature of the conducted SE.

3. CONDITIONS OF THE EXPERIMENT, EQUIPMENT, AND OBSERVATIONAL METHOD

The conditions of the SE session conducted on April 17, 2013 were the following. Solar and geophysical conditions: very quiet state of the geomagnetic field, the solar activity index $F10.7 = 107.1$, the electron concentration maximum (5.87×10^5 cm^{-3}) was located at a height of 301 km. Weather conditions were suitable for photometer measurements. The calculated conditions were: CS orbit height was 412 km, the duration of ACE operation was 9 s (13.24:38–13.24:47 UT), which corresponds to burning 9 kg of fuel, and the direction of the exhausted jets was against the radio beam of IISR. The optical equipment was located at 120 km from IISR.

The assumed molar percentage of the exhaust gases was:

$H_2O = 2.932 \times 10^{-1}$, $N_2 = 2.676 \times 10^{-1}$, $CO = 1.932 \times 10^{-1}$, $H_2 = 1.877 \times 10^{-1}$, $CO_2 = 4.946 \times 10^{-2}$, $H = 8.524 \times 10^{-3}$, $NO = 3.392 \times 10^{-4}$, $OH = 2.853 \times 10^{-5}$, $O_2 = 2.744 \times 10^{-5}$, $O = 1.391 \times 10^{-5}$, $N = 5.376 \times 10^{-8}$. Gas velocity, density, and temperature were 2.8 km/s, 2.7×10^{-3} kg m^{-3}, and ~590 K, respectively.

The following optical equipment was used in the experiment. The SATI-1M spectrometer (http://atmos.iszf.irk.ru/ru/data/spectr), the wide-angle color CCD camera (http://atmos.iszf.irk.ru/ru/data/color), the two-channel photometer with a possibility of exact positioning into the given point of the celestial sphere, and the wide-angle optical system KEO Sentinel to observe the atomic oxygen line [OI] 630 nm. The equipment was located at the Geophysical Observatory (GPO) of ISTP SB RAS (52° N, 103° E).

The SATI-1M spectrograph is mounted on the base of the ISP-51 spectrograph (developed by LOMO) and color CCD matrix SONY ICX285AQ (VIDEOSKAN-285 camera developed by NPO VIDEOSKAN, http://videoscan.ru/). In order for the matrix dimensions to agree with the dimensions of the spectra in the focal plane, a Gelios-40 objective ($F = 85$ mm, 1 : 1.5) is installed as a camera objective. To illuminate the input slit of the spectrometer, a Jupiter-3 objective ($F = 50$ mm, 1 : 1.5) is used. The working spectral range of the spectrograph is 400–700 nm, and the time of spectra exposition is 260 s. The optical axis of the SATI-1M spectrograph was oriented northward with a zenith angle of ~67°.

The FILIN-1C camera is collected on the basis of a cooled color CCD matrix KODAK KAI-11002 (camera VIDEOSKAN-11002 developed by the VIDEOSKAN NPO, http://videoscan.ru/). The Mir-20 objective (focal distance of 20 mm, relative aperture 1 : 3.5) is used as an input objective. The camera put into a case with thermal stabilization is installed at the turning turret, and oriented to the northern part of the sky, at the region of Earth's pole. The angular field of view of the FILIN-1C camera is ~90°. The exposure time is ~300 s. The matrix resolution is 4004 × 2671 pixels.

The wide-angle optical system KEO Sentinel to observe the atomic oxygen line [OI] 630 nm is produced by KEO Scientific Ltd. (http://keoscientific.com/space-science-imagers.php#SENTINEL). The field of view of the optical system is 145°. The half-width of the interference filter (630 nm) is ~1 nm. The optical system is directed to the zenith. The exposure time is 30 s. The binning is 4. Frames are made continuously, one after another. The technical pause between the frames is ~1 s.

The two-channel photometer is installed in the astronomical dome and directed into the given point of the sky with the help of the equatorial installation HEQ5 PRO. The photometer is used to register the intensity of the atomic oxygen emissions 557.7 nm (channel sensitivity is 3×10^{-6} erg cm^{-2} s^{-1}) and 630.0 nm (channel sensitivity is 1×10^{-6} erg cm^{-2} s^{-1}). The field of view of the photometer is ~4°. The time resolution is 10 ms.

The solar zenith angle during the operation of ACE was ~−100°, that is, the observations were made during nautical twilight. The orbit of the *Progress M-17M* CS in the given session did not fall into the field of view of the SATI-1M spectrometer and wide-angle color CCD camera. These devices are used for conducting patrol observations of the natural (background) night airglow and for monitoring solar and geophysical disturbances requiring the fixed orientation of these devices.

4. OBSERVATIONAL RESULTS AND DISCUSSION

As the ACE was operating, the height of the lower boundary of the atmosphere in the zenith still illuminated by the Sun was ~140 km. Thus, CS and its surroundings were illuminated by direct solar radiation. This fact was favorable for the realization of the mechanism of light scatter from gas and dispersed components of the exhaust jets of ACE. On the other hand, such conditions have already made it possible to reveal airglow in order to estimate the optical effects that could be observed in atmospheric modification [14],

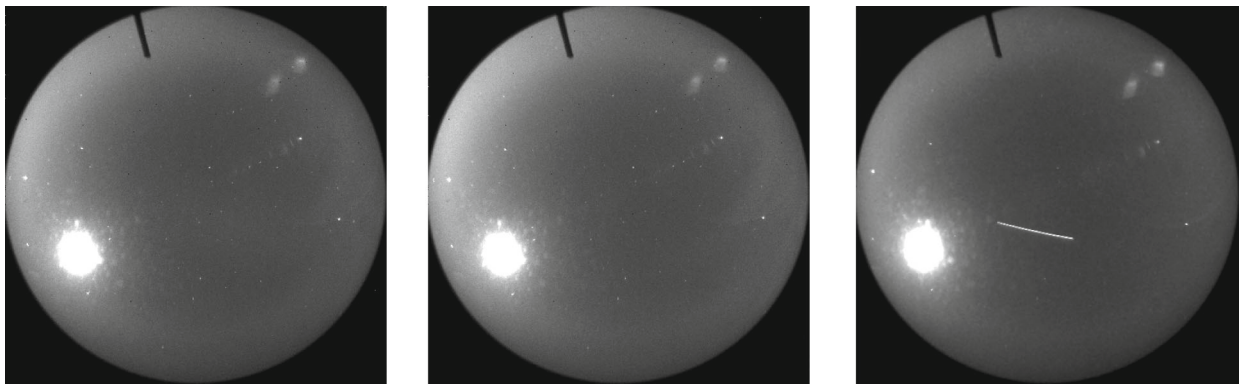

Fig. 1. Initial images obtained by the CCD camera in 630-nm emission.

in particular, in the emission lines of atomic oxygen 557.7 and 630 nm.

Figure 1 shows the particular initial images obtained by the CCD camera in the 630-nm emission range at various observational moments (13.23:29, 13.26:35, and 13.37:25 UT, respectively). The first two frames correspond to the time prior and after the operation of ACE, whereas the last frame corresponds to the time of flight of the *International Space Station*. The bright spot in the lower left-hand side of the photos is an image of the Moon broadened due to the blooming effect.

The images were processed using the following method. Before the measurements, the background was recorded with the closed lens cap. In further processing, an averaged background frame (averaged over 5 frames) was used. Background values were subtracted from all the frames under consideration at the first stage of the processing. Then a reference frame, registered before the switching-on of ACE, was chosen out of the set of photos. The reference frame was subtracted from the following analyzed frames for smooth compensation of the background airglow. As a result, changes in the emission brightness caused by rapid processes (switching-on of ACE, trails of spacecraft and meteors, changes in the atmospheric transparency, etc.) remained on the image. To smooth noise, current median filtration over the frame field was used. This processing method is described in more detail in [3].

Figure 2 shows the data of observations by the all-sky camera in the 630-nm line in the period of operation of ACE, obtained using the method described above. The time of the beginning of exposition of the corresponding frames is indicated.

Beginning with the frame with the exposition at 13.24:31 UT, including the time of ACE operation, southeast of the image center (zenith), an emission region of enhanced intensity is detected; at subsequent moments of time it expands along and across the CS flight trajectory. The total time of the observation of the enhanced intensity region was ~5 min. According to the preliminary estimates, at the CS orbit height of ~400 km, the velocity of the emission region expansion during the first 60 s after ACE switching-on was ~7 and ~3.5 km/s along the CS orbit and across it, respectively. The observed maximum dimensions of the region were registered ~120–150 s later and were ~350 and ~250 km along the orbit and across it, respectively.

Figure 3 shows the time dependence of the emission intensity in the center of the disturbed region relative to the surrounding background, obtained using processed images of the CCD camera in the 630 nm emission. Relative to the surrounding background, the increase in the brightness of the disturbed part of the image in the maximum was ~20%. Bearing in mind that the natural intensity of the atmospheric emission in the zenith at the beginning of night usually has a value of 200–300 R (this agrees with the data of measurements of the 630 nm emission intensity by the SATI-1M spectrograph in the northern part of the sky, presented in Fig. 4), one can estimate the equivalent maximum intensity of the disturbance by a value of ~40–60 R in the spectral passband of the interference filter of 2 nm.

During the operation of ACE, the illumination level was too high for the two-channel photometer. The photometer entered the operational regime ~10 min after the flight of the *Progress M-17M* CS.

The observational data presented in Figs. 1–3, the geophysical conditions of the observations (twilight), and the characteristic life-times and spatial dimensions of the optical formation make it possible to refer the observed optical effect preliminarily to one of the main types of optical phenomena mentioned in some papers (see, for example, [1, 6]), the mechanism of which is related to scattering of the sunlight from products of CS operation. It was noted in [7] that the presence of dispersed particles is the most important factor governing the intensity of such effects. The dispersed particles are formed as a result of the conden-

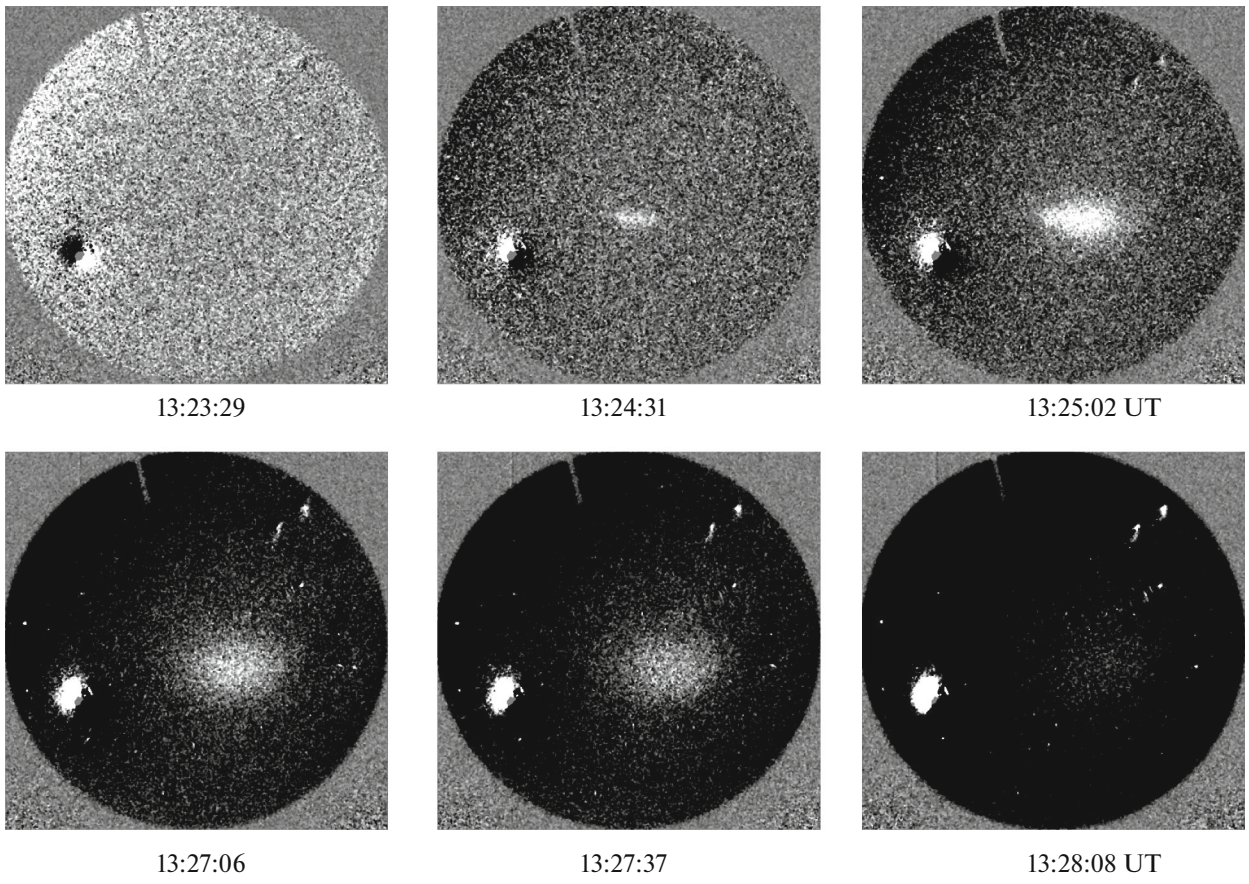

Fig. 2. Sequence of processed frames of the CCD camera images in 630 nm-emission. The time of ACE operation was 13.24:38—13.24:47 UT.

sation of water vapor and carbon dioxide in the exhaust jet of engines.

At the same time, one should not exclude the possibility of the interpretation of the observed effect by a modification of the ionosphere in the increased intensity region and by occurrence of an additional emission in the atomic oxygen line [OI] 630 nm [14]. The increase in the emission brightness beginning from 13.25:02 UT as compared to the emission brightness during the ACE operation could serve as a confirmation of this statement. The expansion of the initial emission region with a simultaneous increase in the brightness may be caused by a change in the reflective characteristics of the ACE exhaust products or by the appearance of an additional emission source.

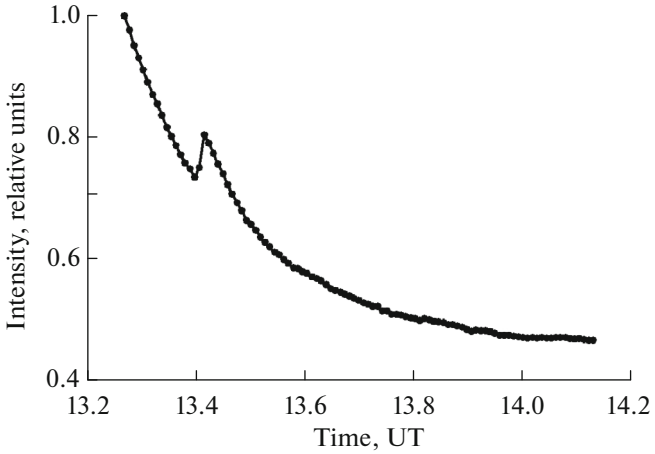

Fig. 3. Time dependence of brightness of disturbed region relative to surrounding background.

Supersonic velocities (~1–4 km/s) of the expansion of optical formations in the upper atmosphere during the ACE operation have also been mentioned earlier [2, 16]. It is believed that diffusion is the mechanism of the propagation of ACE exhaust products at heights of the upper atmosphere. In the region governed by the diffusion process, the ACE exhaust products, apart from the usual process of mixing with the atmosphere, may lead also to changes in aeronomical processes at injection heights and be accompanied by a modification of the ionosphere, including changes in airglow in the main emission lines and bands [1].

Figure 4 shows the data of observations of airglow in the emission lines of atomic oxygen [OI] 557.7 nm (the emission height is ~85–115 km) and [OI] 630.0 nm

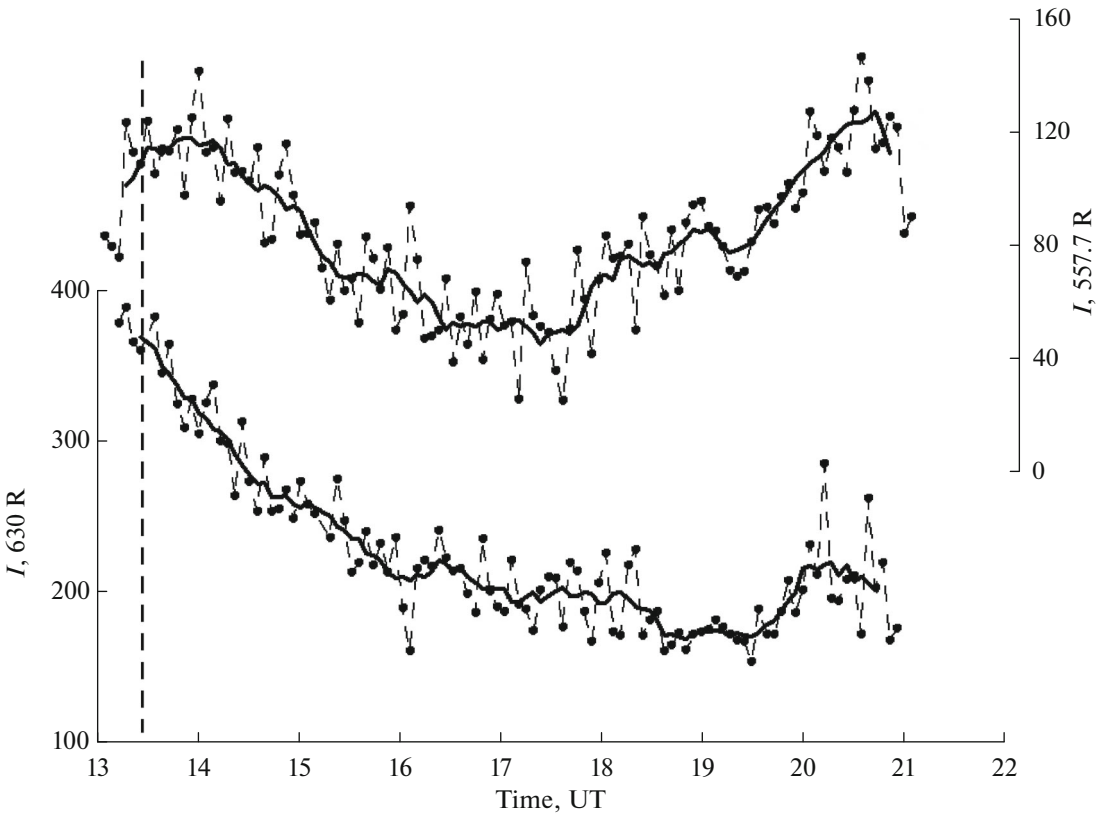

Fig. 4. Variations in [OI] 557.7- and 630.0-nm emission lines during night of April 17/18, 2013.

(~180–300 km) during the night of April 17/18, 2013. These are dominating emissions registered in experiments on ionospheric modification during the ACE operation [14]. The region of registration of airglow was located at distances of ~235 km (for the height of the maximum emission of the 557.7 nm line) and ~600 km (630.0 nm) northward of the zenith, respectively. The vertical dashed line in Fig. 4 shows the moment of the switching-on of ACE. The preliminary analysis of the variations in the intensity of the 557.7 and 630 nm emissions does not make it impossible to reveal disturbances substantially exceeding the natural variations in these emissions after the switching-on of ACE. This fact makes it possible to draw a preliminary conclusion on the absence of the large-scale modification of the ionosphere in the studied session of SE. Apparently, this is related to the fact that either the region of diffusion of the ACE exhaust products had limited dimensions, or the possible effect of ionospheric modification at large distances was negligible, in particular, due to the relatively small mass of the injected exhaust products.

CONCLUSIONS

The analysis of the data of optical observations during the night of April 17/18, 2013, when Radar-Progress Active SE was conducted, makes it possible to draw the following preliminary conclusions:

1. During the operation of the ACE of the *Progress M-17M* CS, a region of enhanced intensity of emissions, presumably related to the scatter of the twilight solar radiation at the products of the ACE operation in the CS orbit and, probably, to the appearance of additional emission in the atomic oxygen [OI] 630 nm line, was registered. The maximum observed dimensions of the emission region were ~350 and ~250 km along the orbit and across it, respectively. The velocity of the expansion of the emission region at the first moments after the beginning of ACE operation was ~7 and ~3.5 km/s along the orbit and across it, respectively. The maximum intensity of the disturbed region is estimated to be a value equivalent to ~40–60 R within the spectral band of 2 nm.

2. No optical manifestation, which would exceed the natural variations in the brightness of the night airglow and be related to possible large-scale modification of the ionosphere, was detected in natural variations in the brightness of the nightglow and related to possible large-scale modification of the ionosphere was detected.

ACKNOWLEDGMENTS

The work was performed in the scope of the No. NSH-2942.2014.5 grant of the President of RF of state support for the leading scientific schools of the RF, with the use of the scientific equipment of the Angara CUC of ISTP SB RAS and with the support of the Russian Foundation for Basic Research, projects Nos. 13-05-00456-a and 13-02-00957-a.

REFERENCES

1. Adushkin, V.V., Kozlov, S.I. and Petrov, A.V., *Ekologicheskie problemy i riski vozdeistviya raketno-kosmicheskoi tekhniki na okruzhayushchuyu sredu: Spravochnoe posobie* (Ecological Problems and Risks of the Environmental Impact of Space Rocket Technology: A Reference Book), Moscow: Ankil, 2000.
2. Vetchinkin, N.V., Granitskii, N.V., Platov, Yu.V., and Sheichue, A.I., Optical phenomena in the near-Earth environment under the operation of engine units of rockets and satellites. 1. Ground-based and satellite observations of artefacts at rocket launching, *Kosm. Issl.*, 1993, vol. 31, no. 1, pp. 93–100.
3. Grach, S.M., Klimenko, V.V., Shindin, A.V., et al., Airglow during ionospheric modifications by the sura facility radiation. Experimental results obtained in 2010, *Radiophys. Quantum Electron.*, 2012, vol. 55, no. 1, pp. 33–50.
4. Karlov, V.D., Kozlov, S.I., and Tkachev, G.N., Large-scale disturbances in the ionosphere arising from flights of rockets with active engine (a review), *Kosm. Issled.*, 1980, vol. 181, no. 2, pp. 266–277.
5. Mikhalev, A.V. and Ermilov, S.Yu., Observations of disturbances in ionospheric emission layers arising at cosmic system flights, in *Issledovaniya po geomagnetizmu, aeronomii i fizike Solntsa* (Studies on Geomagnetism, Aeronomy, and Solar Physics), Novosibirsk: SO RAN, 1997, no. 107, pp. 206–217.
6. Platov, Yu.V., Kulikova, G.N., and Chernous, S.A., Classification of gas-dust structures in the upper atmosphere associated with the exhausts of rocket-engine combustion products, *Cosmic Res.*, 2003, vol. 41, no. 2, pp. 153–158.
7. Platov, Yu.V., Semenov, A.I., and Filippov, B.P., Condensation of combustion products in the exhaust plumes of rocket engines in the upper atmosphere, *Geomagn. Aeron. (Engl. Transl.)*, 2011, vol. 51, no. 4, pp. 550–556.
8. Khakhinov, V.V., Potekhin, A.P., Lebedev, V.P., et al., Radiophysical methods for the diagnostics of ionospheric disturbances generated by onboard engines of the Progress transport cargo unmanned spacecraft: Algorithms, instruments, and results, in *Trudy konferentsii "Zondirovanie zemnykh pokrovov s sintezirovannoi aperturoi", 06–10 sentyabrya 2010 g., Ulan-Ude* (Proceedings of the Conference "Sounding of Terrestrial Covers with Synthesized Aperture," September 6–10, 2010, Ulan-Ude), 2010, pp. 555–571.
9. Khakhinov, V.V., Potekhin, A.P., Lebedev, V.P., et al., Results of remote sounding of ionospheric disturbances during active space experiments "Radar-Progress," *Sovrem. Probl. Distantsionnogo Zondirovaniya Zemli Kosmosa*, 2012, vol. 9, no. 3, pp. 199–208.
10. Khakhinov, V.V., Potekhin, A.P., Lebedev, V.P., et al., Some results of "Plasma-Progress" and "Radar-Progress" active space experiments, in *Vestn. Sib. Gos. Aerokosm. Univ. im Akad. M. F. Reshetneva*, 2013, no. 5, pp. 160–163.
11. Khakhinov, V.V., Kushnarev, D.S., Podlesnyi, A.V., et al., Radiophysical effects of the operation of a spacecraft engine, *Trudy XXIV Vserossiiskoi nauchnoi konferentsii "Rasprostranenie radiovoln"* (Proceedings of the XXIV All-Russian Scientific Conference "Radio Wave Propagation"), vol. 1, Irkutsk, 2014, pp. 60–66.
12. Khakhinov, V.V., Lebedev, V.A., Medvedev, A.V., and Ratovsky, K.G., Capabilities of the Irkutsk incoherent scattering radar for space debris studies, in *Proceedings of the 5th European Conference on Space Debris, Darmstadt. Germany, 2009*, ESA SP-672.
13. Mendillo, M.J., Hawkins, G.S., and Klobuchar, J.A., A sudden vanishing of the ionospheric f region due to the launch of Skylab, *J. Geophys. Res.*, 1975, vol. 80, no. 16, pp. 2217–2218.
14. Mendillo, M. and Baumgardner, J., Optical signature of ionospheric hole, *Geophys. Res. Lett.*, 1982, vol. 9, no. 3, pp. 215–218.
15. Mikhalev, A.V., Midlatitude airglow during heliogeophysical disturbances, *Geomagn. Aeron. (Engl. Transl.)*, 2011, vol. 51, no. 7, pp. 974–978.
16. Tagirov, V.R., Arinin, V.A., Ismagilov, V.V., and Klimenko, V.V., Unusual optical emission in the atmosphere caused by human activity, in *Proceedings of the 22nd European Meeting on Atmospheric Studies by Optical Methods, Nurmijarvi, Finland, 1995*, p. 7.
17. Lebedev, V.P., Khakhinov, V.V., Gabdullin, F.F., et al., Radiosounding-based study of the characteristics of the plasma environment of low-orbit spacecrafts, *Kosmonavtika Raketostroenie*, 2008, no. 1, pp. 51–60.
18. Potekhin, A.P., Khakhinov, V.V., Medvedev, A.V., et al., Active space experiments with the use of the transport spacecraft "Progress" and Irkutsk IS Radar, Moscow, Russia, in *Progress in Electromagnetics Research Symposium Proceedings*, 2009, pp. 223–227.

Translated by A. Danilov